RF/FSO SYSTEM IN K-μ/IG FADING ENVIRONMENT

[1*]Vartika Shukla, [2]J.P. Pandey and [3]Chitranjan Gaur
[1]Research Scholar, Department of Electronics and Communication Engineering MUIT, Lucknow, Uttar Pradesh, India
[2]Research Co-Supervisor, Vice Chancellor MMMUT, Gorakhpur, Uttar Pradesh, India
[3]Research Supervisor, Director SVNIT, Lucknow, Uttar Pradesh, India
vartika.shukla17@gmail.com

ABSTRACT
FSO has gotten a lot of attention because it has very high data rates, can be used without a licence, and can be set up quickly. Aerosol scattering from rain, fog, snow, and other bad weather conditions is one problem that makes it hard to use in real life. Wind loads cause a building to sway. Other things that could cause damage are weak earthquakes and thermal expansion. Turbulence in the air is another big problem in the FSO system. When the refractive index changes, the received signal changes quickly. This is because the temperature and pressure are not all the same. This makes refractive prisms with different sizes and indices of refraction. Eventually, random phases and changes in amplitude (called "scintillation") hurt the performance of FSO links.

Keywords: FSO, backbone network, faded channel, Log normal distribution, ergodic capacity.

I. INTRODUCTION
FSO systems [1] are better than RF systems because they have high bandwidth, high security, low power consumption, and can communicate up to several kilometres away. FSO is interesting because it can transmit without a licence, is easy to set up, and is cheap], and because it has narrow beams that make it very direct. This makes it even more interesting to meet the needs of future wireless systems.

II. REVIEWS & GOAL
The goal of the RF/FSO system is to link the last-mile access (FSO) to the main backbone network (RF) [4]. Hybrid RF/FSO Systems use the best parts of both RF links and FSO links. RF lets you talk without line-of-sight, while FSO lets you send data quickly and with little delay. The RF/FSO system connects the last mile at a low cost, with high reliability and a faster data rate [5]. In [6], the authors looked at how well an RF/FSO system based on Meijer's G function worked when Gamma-Gamma (GG) faded channels were present. [7] looks at the AF-based relaying protocol, while [4] and [8] look at the DF-based RF/FSO network. Sampling, amplifying, and retransmitting aren't easy in the AF scheme [9]. It amplifies both the desired signal and the noise [100], while the DF protocol re-encodes the signal after decoding and amplifying it [9], before sending it to its destination. So, DF makes it possible for the communication rates of SR and RD links to be changed. Decode-and-forward systems can also be made to work better by using different encoding schemes [11].

Relaying increases the amount of data that can be sent and covers a larger area. [12] was the first person to talk about RF and FSO-based two-hop relaying in an asymmetric environment. Asymmetric systems are better because they take into account different fading models for each hop. In the real world, the signals that are received are sent through different fading scenarios [13]. [6] and [13] thought about an environment with asymmetric or mixed fading.

Log-normal distribution (LN), which is often used to model weak turbulences [14], was used in the past to model large-scale fading. It also models turbulence when the receiver's opening is bigger than the length of the fluctuations [15]. After that, Gamma distribution was created to describe the effect of shadowing more accurately. Kolmogorov-Smirnov (KS) statistical tests [19] and [16] show that LN distribution is a better replacement for Gamma distribution than IG distribution. This is because IG distribution is easier to work with from an analytical point of view. In FSO communication, IG distribution gives a good approximation of LN distribution for different kinds of turbulence. The cumulant function of the IG distribution is the opposite of the cumulant function of the normal distribution.

Rayleigh, Nakagami-q (Hoyt), Nakagami-m, and Weibull are well-known distributions for LOS communication that can be used to model small-scale fading. For nLOS communication, the Nakagami-n (Rice) model is well-known. The Weibull, Gamma, Exponential, One-sided Gaussian, Nakagami-m, and Rayleigh distributions are all special cases of the generalised Gamma (Stacy) distribution, which is also called the a- distribution [18, 19]. Also, h- and a-, [20]–[23], model small-scale fading and are again groups of many other distributions. In a non-homogeneous environment, the h- distribution is a good way to describe how a signal acts. In a homogeneous environment, on the other hand, the k- distribution is used.

To make an accurate model of a fading environment in real time, both multipath and shadowing effects should be taken into account at the same time. Malaga (M) is different from many other models because of its coupled-to-LOS component and the effect it has. It is a new generic propagation model proposed by [18], which is widely accepted for modelling of weak to strong atmospheric turbulences, with the limitation that the amount of fading parameter (b) is only defined for natural numbers [18]. Malaga distribution makes it easy to get to the most common Gamma-Gamma (GG) distribution. Gamma, not LN distribution, is used to model changes in the GG distribution that happen on a large scale. But for LN distribution, the Gamma distribution is not a good approximation when the variance is large [24, 25].

A new type of distribution called k-/Inverse Gaussian is a flexible fading model that can accurately simulate how fading happens in real time. As special cases, [19] includes the Rice (Nakagami-n)/IG, one-sided Gaussian/IG, Nakagami/IG, and Rayleigh/IG distributions. It can be used to model turbulences that are moderate to strong [19]. After doing a thorough search of the literature, it was found that k-/Inverse Gaussian distribution on RF/FSO system has not been talked about yet. When it comes to modelling weak turbulence, the IG distribution is better than the Gamma distribution [96]. The performance of an RF/FSO system based on the DF and AF approaches is looked at in [4] and [17], with the assumption that the RF link has a Nakagami-m distribution and the FSO link has a Gamma Gamma distribution. In this chapter, we look at the RF/FSO network. The first link has a Rayleigh distribution, and the second link has a k-/Inverse Gaussian distribution.

III. SYSTEM MODEL

In Fig. 2.1, we look at a dual-hop asymmetric RF/FSO system based on the DF relaying protocol. The source (S) and the destination (D) are at a distance of nLOS from each other. It is assumed that both the destination and the relay are set up on high-rise buildings that are in line of sight of each other. In this system, S and D talk to each other through a relay (R).

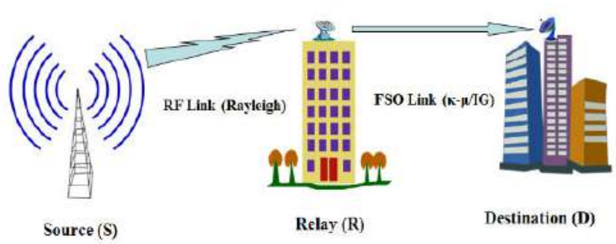

Figure 2.1 Dual-hop RF/FSO based model

In an asymmetric wireless channel, the S R RF link is thought to have a Rayleigh distribution, while the R D FSO link is thought to have a k /Inverse Gaussian distribution. After getting an RF signal from the source, the relay changes it into an optical signal, where "h" is the optical conversion ratio. The SNR of the S R link is given by the instantaneous SNR, g S;R. The equation for the RF signal at R, given by y, is

$$ys,R = h_{s,}R^{x} + n^{1} S, R, \quad (2.1)$$

where x defines the RF signal transmitted by S with fading gain, $h_{S,R}$. The AWGN noise between S-R link is denoted by n^1 S, R . The SNR of first hop is given be

$$\gamma_{S,R} = \Omega_{S,R}|h_{S,R}|^2/\ N_0 = |h_{S,R}|^2/\ \bar{\gamma},$$

where the average SNR and average energy of S-R link are denoted by $\bar{\gamma}$ and $\Omega_{S,R}$ respectively. N_0 denotes the variance of AWGN noise. The S-R link is considered to be Rayleigh distributed and its PDF is given by [103]

$$f_{\gamma SR}(\gamma) = \frac{1}{\bar{\gamma}} \exp\left(-\frac{\gamma}{\bar{\gamma}}\right) \qquad (2.2)$$

The instantaneous SNR of second hop is given by $\gamma_{R,D}$. The signal, $\gamma_{R,D,}$ at destination D can be written as

$$\gamma_{R,D,} = \eta I_{\tilde{x}} + n^1_{R,D,} \qquad (2.3)$$

where $\tilde{x}$ is the signal estimated at R and $n^1_{R,D}$ AWGN variance. I denotes intensity of irradiance. The instantaneous electrical SNR of second hop is $\gamma_{R,D,} = (\eta I)^2/N_0$. The average electrical SNR, $\tilde{\gamma}$, of both the hops is assumed similar in order to make the analysis simpler. The expression of $\tilde{\gamma}$ is given [115] as

$$\tilde{\gamma} = \frac{(\eta E[I])^2}{N_0},$$

where E [.] represents the expectation operator. γ_{DF} is the equivalent SNR of the DF based link S-R-D-, which is given by $\gamma_{DF} = \min(\gamma_{S,R}, \gamma_{R,D})$. It specifies the minimum of the two SNRs, $\gamma_{S,R}$ and $\gamma_{R,D}$ of both the hops. The PDF of the proposed DF based model is stated as

$$f_\gamma(\gamma) = f_{\gamma S,R}(\gamma) + f_{\gamma R,D}(\gamma) - f_{\gamma S,R}(\gamma)F_{\gamma R,D}(\gamma) - f_{\gamma R,D,}(\gamma)F_{\gamma S,R}(\gamma), \qquad (2.4)$$

where $F_{\gamma S,R}$ denotes CDF between S and R link.

IV. CHANNEL STATISTICS

The MGF-based expressions make it easier and faster to do analytical work. The MGF of the model being proposed is [23].

$$M_\gamma(s) = \int_0^\infty f_\gamma(\gamma)\exp(-s\gamma)d\gamma$$

Thereafter, we substitute the value of $f_\gamma(\gamma)$ from eq. (2.4) to eq. (2.7), to yield MGF as

$$M_\gamma(s) = \int_0^\infty f_{\gamma S,R}(\gamma) + f_{\gamma R,D}(\gamma) - f_{\gamma S,R}(\gamma)F_{\gamma R,D}(\gamma)F_{\gamma S,R}(\gamma) \times \exp(-s\gamma)d\gamma.$$

Further, eq. (2.8) can be written as

$$M_\gamma(s) = I_1 + I_2 - I_3 - I_4,$$

Where

$$I_1 = \int_0^\infty f_{\gamma S,R}(\gamma)\exp(-s\gamma)d\gamma$$

$$I_2 = \int_0^\infty f_{\gamma R,D}(\gamma)\exp(-s\gamma)d\gamma$$

$$I_3 = \int_0^\infty f_{\gamma S,R}(\gamma)F_{\gamma R,D}(\gamma)\exp(-s\gamma)d\gamma,$$

and

$$I_4 = \int_0^\infty f_{\gamma R,D}(\gamma)F_{\gamma S,R}(\gamma)\exp(-s\gamma)d\gamma,$$

After solving I_1 in eq. (2.10), we get

$$I_1 = \left(\frac{1}{1+\bar{\gamma}s}\right)$$

Moreover, the CDF, $F_{\gamma S,R}$, of S-R link is expressed as

$$F_{\gamma S,R} = 1 - \exp\left(-\frac{\gamma}{\bar{\gamma}}\right)$$

After substituting $F_{\gamma S,R}$ in I_4eq. (2.13) reduces to

$$I_4 = \int_0^\infty f_{\gamma R,D}\exp(-s\gamma)d\gamma - \int_0^\infty f_{\gamma R,D}\exp\left(-\left(s+\frac{1}{\bar{\gamma}}\right)\gamma\right)d\gamma,$$

Henceforth, we substitute the values ofI_4 from eq. (2.13) andI_1 in$M_\gamma(s)$, we find that the first term ofI_4 gets cancelled withI_2.

Henceforth, $M_\gamma(s)$ reduces to

$$M_\gamma(s) = \frac{1}{1+\bar{\gamma}s}$$
$$-\int_0^\infty\left(f_{\gamma S,R}(\gamma)F_{\gamma R,D,}(\gamma)\exp(-s\gamma) - f_{\gamma R,D}\exp\left(-\left(s+\frac{1}{\bar{\gamma}}\right)\gamma\right)\right)d\gamma.$$

By using change of variable method, we solve $M_\gamma(s)$ in eq. (2.15). In addition, the following relations are plugged to solve eq. (2.15) to derive the final expression. The expressions of $f_{\gamma R,D,}$ and $F_{\gamma R,D,}$ from eq. (2.5) and eq. (2.6) respectively, are substituted in eq. (2.15). However, the Bessel functions,

$$K_{\mu+i+\frac{1}{2}}\left[\sqrt{\frac{\mu(1+k)\gamma}{2\theta\bar{\gamma}}+\frac{\lambda^2}{4\theta^2}}\right]$$

and

$$K_{\mu+i-k+1/2}\left(b\sqrt{\alpha+\beta\gamma}\right)$$

in PDF and CDF of second link respectively, are obtained using the relation [110, eq. (8.485)] given as

$$K_v(z) = \frac{\pi}{2}\left(\frac{I_{-v}(z)-I_v(z)}{\sin(v\pi)}\right)$$

Where

$$I_v(x) = \left(\frac{x}{2}\right)^v\sum_{k=0}^{\infty}\frac{1}{\Gamma(k+1)\Gamma(v+k+1)}\left(\frac{x}{2}\right)^{2k}$$

We solve the integral obtained by applying Binomial expansion, using the relation [118,eq.(3.381.3)]

$$\int_u^\infty x^{v-1}\exp(-\mu x)dx = \mu^{-v}\Gamma(v,\mu u)$$

V. PERFORMANCE ANALYSIS:

1 ERGODIC CAPACITY:

Based on unified MGF, the relation can be used to figure out the ergodic capacity of proposed model [28].

$$C_{avg} \simeq \frac{B}{log(2)} \sum_{n=1}^{N} v_n Ei(-s_n) \left[\frac{d}{ds} M_{\gamma}(s) \right]_{s \rightarrow s_n},$$

Where B is the channel's bandwidth, N is a positive number, and Ei () is the exponential integral function [29, eq. 6.15.2]. v n and s are [28] coefficients, which are defined as

$$v_n = \frac{\pi^2 sin(((2n-1)/2N)\pi)}{4Ncos^2((\pi/4)cos((((2N-1)/2N)\pi)+(\pi/4))}$$

and

$$s_n = tan\left(\frac{\pi}{4}cos\left(\left(\frac{2n-1}{2N}\right)\pi\right)+\frac{\pi}{4}\right).$$

Eq. (2.40) represents the differentiation of MGF, $M_{\gamma}^{'}(s)$, where we substitute $\Theta = \mu + i - k$.

$$\begin{aligned}
M_{\gamma}^{'}(s) = & \left\{ \frac{-\bar{\gamma}}{(1+\bar{\gamma}s)^2} \right\} + \sum_{i=0}^{p} A(i) \sum_{k=1}^{\mu+i} B(i,k) \sum_{j=0}^{\Theta} \binom{\Theta}{j} (-\alpha)^j \\
& \times \left[\sum_{t=0}^{\infty} \frac{\alpha}{\beta} \left[\left\{ \frac{r^{(-\Theta+2t-\frac{1}{2})} \Gamma\left(-j+t+\frac{1}{2}, \left(\frac{s\bar{\gamma}+1}{\bar{\gamma}\beta}\right)\alpha\right)}{\Gamma(t+1)\Gamma(-\Theta+t+\frac{1}{2})} \left(\frac{s\bar{\gamma}+1}{\bar{\gamma}\beta}\right)^{(j-t-\frac{1}{2})} \right\} \right. \right. \\
& \left. - \left\{ r^{(\Theta+2t+\frac{1}{2})} \left(\frac{s\bar{\gamma}+1}{\bar{\gamma}\beta}\right)^{-(\Theta-j+t+1)} \frac{\Gamma\left(\Theta-j+t+1, \left(\frac{s\bar{\gamma}+1}{\bar{\gamma}\beta}\right)\alpha\right)}{\Gamma(t+1)\Gamma(\Theta+t+\frac{3}{2})} \right\} \right] \\
& + \sum_{t=0}^{\infty} \left[\left\{ \left(j-t-\frac{1}{2}\right) \left(\frac{s\bar{\gamma}+1}{\bar{\gamma}\beta}\right)^{(j-t-\frac{3}{2})} r^{(-\Theta+2t-\frac{1}{2})} \frac{\Gamma\left(-j+t+\frac{1}{2}, \left(\frac{s\bar{\gamma}+1}{\bar{\gamma}\beta}\right)\alpha\right)}{\Gamma(t+1)\Gamma(-\Theta+t+\frac{1}{2})} \right\} \right. \\
& - \left\{ \frac{r^{(-\Theta+2t-\frac{1}{2})}}{\left(\frac{s\bar{\gamma}+1}{\bar{\gamma}}\right)} \frac{\alpha^{(-j+t+\frac{1}{2})} \exp\left(-\left(\frac{s\bar{\gamma}+1}{\bar{\gamma}\beta}\right)\alpha\right)}{\Gamma(t+1)\Gamma(-\Theta+t+\frac{3}{2})} \right\} \\
& + \left\{ \frac{\left(\frac{s\bar{\gamma}+1}{\bar{\gamma}\beta}\right)^{(-\Theta+j-t-2)} (-\Theta+j-t-1) r^{(\Theta+2t+\frac{1}{2})} \Gamma\left(\Theta-j+t+1, \left(\frac{s\bar{\gamma}+1}{\bar{\gamma}\beta}\right)\alpha\right)}{\Gamma(t+1)\Gamma(\Theta+t+\frac{3}{2})} \right\} \\
& \left. \left. + \left\{ \frac{r^{(\Theta+2t+\frac{1}{2})}}{\left(\frac{s\bar{\gamma}+1}{\bar{\gamma}}\right)} \frac{\alpha^{(\Theta-j+t+1)} \exp\left(-\left(\frac{s\bar{\gamma}+1}{\bar{\gamma}\beta}\right)\alpha\right)}{\Gamma(t+1)\Gamma(\Theta+t+\frac{3}{2})} \right\} \right] \right] + \sum_{i=0}^{p} A(i) D(i) \sum_{j=0}^{\mu+i-1} \binom{\mu+i-1}{j} \qquad (2.40) \\
& \times (-\alpha)^j \left[\sum_{t=0}^{\infty} \frac{1}{\beta} \left[\left\{ r^{(-\mu-i+2t-\frac{1}{2})} \frac{\Gamma\left(-j-t+\frac{5}{2}, \left(\frac{s\bar{\gamma}+1}{\bar{\gamma}\beta}\right)\alpha\right)}{\Gamma(t+1)\Gamma(-\mu-i+t+\frac{1}{2})} \left(\frac{s\bar{\gamma}+1}{\bar{\gamma}\beta}\right)^{(j+t-\frac{5}{2})} \right\} \right. \right. \\
& \left. - \left\{ \frac{r^{(\mu+i+2t+\frac{1}{2})} \left(\frac{s\bar{\gamma}+1}{\bar{\gamma}\beta}\right)^{(-\mu-i+j-t-1)} \Gamma\left(\mu+i-j+t, \left(\frac{s\bar{\gamma}+1}{\bar{\gamma}\beta}\right)\alpha\right)}{\Gamma(t+1)\Gamma(\mu+i+t+\frac{3}{2})} \right\} \right] \\
& + \sum_{t=0}^{\infty} \left[\left\{ \frac{r^{(-\mu-i+2t-\frac{1}{2})} \left(\frac{s\bar{\gamma}+1}{\bar{\gamma}\beta}\right)^{(j+t-\frac{7}{2})} (j+t-\frac{5}{2})}{\beta} \frac{\Gamma\left(-j-t+\frac{5}{2}, \left(\frac{s\bar{\gamma}+1}{\bar{\gamma}\beta}\right)\alpha\right)}{\Gamma(t+1)\Gamma(-\mu-i+t+\frac{1}{2})} \right\} \right. \\
& - \left\{ \frac{r^{(-\mu-i+2t-\frac{1}{2})} \alpha^{(-j-t+\frac{5}{2})} \exp\left(-\left(\frac{s\bar{\gamma}+1}{\bar{\gamma}\beta}\right)\alpha\right)}{\left(\frac{s\bar{\gamma}+1}{\bar{\gamma}}\right) \Gamma(t+1)\Gamma(-\mu-i+t+\frac{1}{2})} \right\} \\
& - \left\{ \frac{\Gamma\left(\mu+i-j+t, \left(\frac{s\bar{\gamma}+1}{\bar{\gamma}\beta}\right)\alpha\right) r^{(\mu+i+2t+\frac{1}{2})} \left(\frac{s\bar{\gamma}+1}{\bar{\gamma}\beta}\right)^{(-\mu+j+t-i-1)} (-\mu-i+j-t)}{\Gamma(t+1)\Gamma(\mu+i+t+\frac{3}{2})} \right\} \\
& \left. \left. + \left\{ \frac{r^{(\mu+i+2t+\frac{1}{2})} \alpha^{(\mu+i-j+t)} \exp\left(-\left(\frac{s\bar{\gamma}+1}{\bar{\gamma}\beta}\right)\alpha\right)}{\left(\frac{s\bar{\gamma}+1}{\bar{\gamma}}\right) \Gamma(t+1)\Gamma(\mu+i+t+\frac{3}{2})} \right\} \right] \right].
\end{aligned}$$

VI. RESULTS AND DISCUSSIONS:

The theoretical plots of the ergodic channel capacity given by equation (2.39), and the BER given by equations (2.42 and 2.43), are made. The line between ergodic capacity and average SNR is shown in Fig. 2.2. Over the capacity of the channel, the effects of k,, q, and l are shown. It has been seen that, for a certain set of values (l = 1.2, = 2, and k = 5), the capacity improves significantly as the value of q goes up. But for different values of k,, and l, there are only small changes in capacity. When q = 1, k doesn't have much of an effect on capacity. To prove it, the analysis is done for k values of 1, 2, 5, and 10. In the same way, there isn't much difference between l and in the plot.

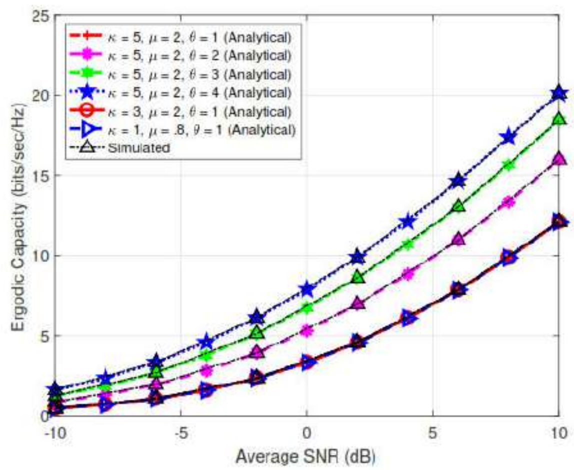

Figure 2.2 Ergodic Capacity of proposed RF/FSO model versus Average SNR

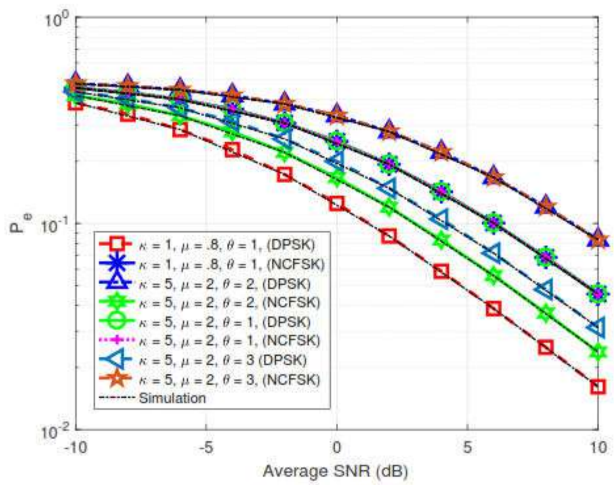

Figure 2.3 BER vs. Average SNR plots from analysis and simulation

Fig. 2.3 shows a graph of the BER against the average SNR, g. Both NCFSK and DPSK look like they have similar BER plots. When the value of g goes up, BER goes down a lot for the specific values of k, q, and a. At l = 1.2 and = 2, the BER has also been looked at. Also, it shows that the BER goes down a lot as q goes from 1 to 3. Figure 2.4 shows how the SER, P, changes with g for the QPSK and BPSK modulation methods. For a certain value of q = 1, and for the two sets of and k that are (1 and 0.8) and (5 and 2), Pe overlaps with itself. k and don't make a big difference in the value of Pe. In both BPSK and QPSK modulation schemes, as q goes up, SER goes down.

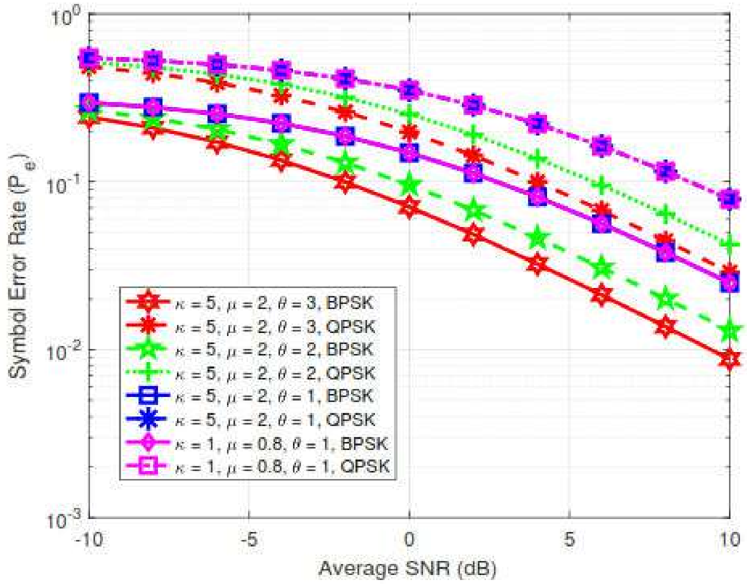

Figure 2.4 The proposed RF/FSO system's symbol error rate compared to the average SNR

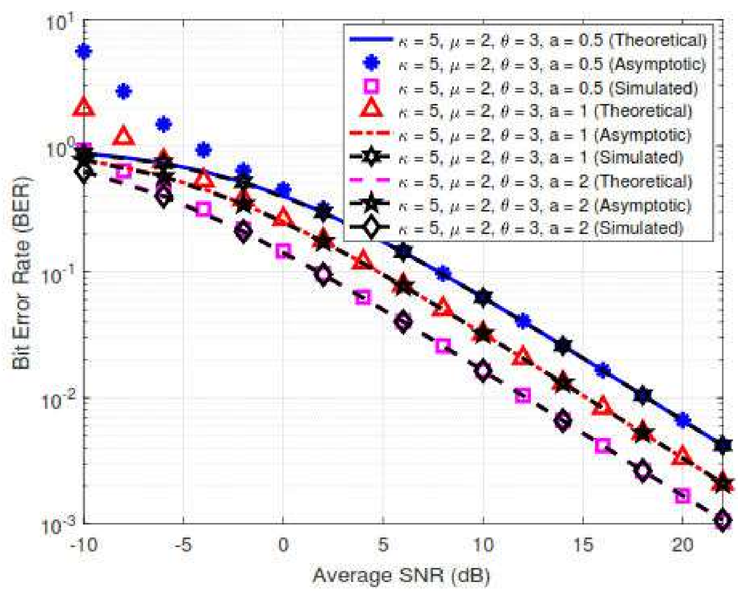

Figure 2.5 Asymptotic behaviour of BER versus Average SNR

Figure 2.5 shows how BER behaves as time goes on. When the SNR is high, the asymptotic results match the analytical results very well. Fig. 2.6 shows how average SNR and l affect the probability of an outage, as shown in eq (2.46). At a value of g = 5 dB that stays the same, OP goes up as k goes down. When =.1 and q = 1, the OP is drawn. It is also clear that, for a given value of k, OP works better when l = 3 than when l = 2.5. k is the ratio of the power of the most important components to the power of the scattered waves [9].

Figure 2.6 shows that as k goes up, so doesOP, while Figure 2.7 shows how changes as l goes up or down. For the OP plots in Fig. 2.7, k = 2 and q = 1 have been taken into account. For the values of l of 3.0 and 3.1, the OP gets better as goes from 0.5 to 0.7.

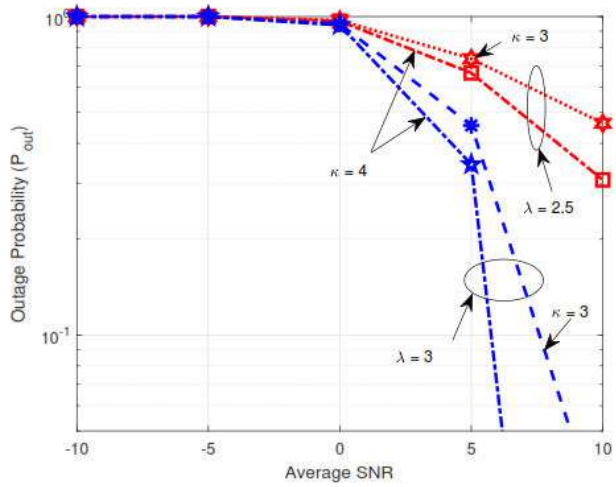

Figure 2.6 OP vs Average SNR for different k and l

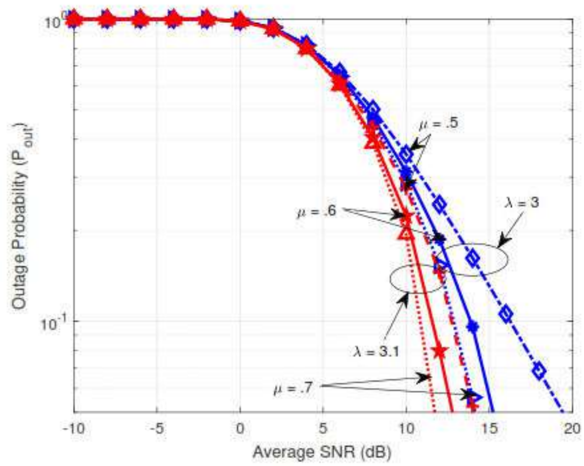

Figure 2.7 OP versus average SNR for proposed RF/FSO system

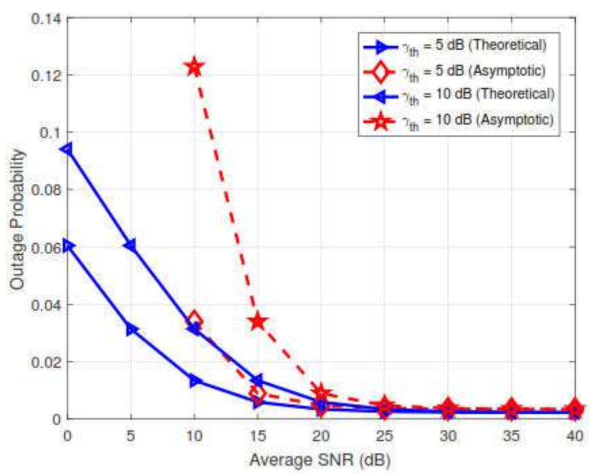

Figure 2.8 Average SNR vs. Asymptotic OP

VII. CONCLUSIONS

The behaviour of the RF/FSO system based on the DF scheme was proposed and looked at in this chapter. It figures out the mathematical expressions of MGF and how it behaves as it gets close to infinity. The asymptotic approximation is also used to look at the special case of MGF. The analytical expressions of MGF are used to figure out the ergodic capacity and BER. The effect of q and average SNR on how well the system works is shown with numbers. Also, the asymptotic expressions of OP for the proposed prove that both analytical expressions are correct. Also, diversity order and coding gain are found to learn more about the system under consideration. The main contribution of this chapter is an analysis of how k-/inverse Gaussian fading works over FSO links.

REFERENCES

[1] S. M. Metev and V. P. Veiko, *Laser Assisted Microtechnology*, 2nd ed., R. M. Osgood, Jr., Ed. Berlin, Germany: Springer-Verlag, 1998.

[2] J. Breckling, Ed., *The Analysis of Directional Time Series: Applications to Wind Speed and Direction*, ser. Lecture Notes in Statistics. Berlin, Germany: Springer, 1989, vol. 61.

[3] S. Zhang, C. Zhu, J. K. O. Sin, and P. K. T. Mok, "A novel ultrathin elevated channel low-temperature poly-Si TFT," *IEEE Electron Device Lett.*, vol. 20, pp. 569–571, Nov. 1999.

[4] M. Wegmuller, J. P. von der Weid, P. Oberson, and N. Gisin, "High resolution fiber distributed measurements with coherent OFDR," in *Proc. ECOC'00*, 2000, paper 11.3.4, p. 109.

[5] R. E. Sorace, V. S. Reinhardt, and S. A. Vaughn, "High-speed digital-to-RF converter," U.S. Patent 5 668 842, Sept. 16, 1997.

[6] (2002) The IEEE website. [Online]. Available: http://www.ieee.org/

[7] M. Shell. (2002) IEEEtran homepage on CTAN. [Online]. Available: http://www.ctan.org/tex-archive/macros/latex/contrib/supported/IEEEtran/

[8] *FLEXChip Signal Processor (MC68175/D)*, Motorola, 1996.

[9] "PDCA12-70 data sheet," Opto Speed SA, Mezzovico, Switzerland.

[10] A. Karnik, "Performance of TCP congestion control with rate feedback: TCP/ABR and rate adaptive TCP/IP," M. Eng. thesis, Indian Institute of Science, Bangalore, India, Jan. 1999.

[11] J. Padhye, V. Firoiu, and D. Towsley, "A stochastic model of TCP Reno congestion avoidance and control," Univ. of Massachusetts, Amherst, MA, CMPSCI Tech. Rep. 99-02, 1999.

[12] *Wireless LAN Medium Access Control (MAC) and Physical Layer (PHY) Specification*, IEEE Std. 802.11, 1997.

[13] Xiangwei Zhou1, Mingxuan Sun, Geoffrey Ye Li, Biing-Hwang(Fred) Juang, "Intelligent Wireless Communications Enabled by Cognitive Radio and Machine Learning"School of EECS, Louisiana State University, Baton Rouge, LA 70803, USA School of ECE, Georgia Institute of Technology, Atlanta, GA 30332, USA;China Communications , December 2018.

[14] Bekele M. Zerihun, Thomas O. Olwal, Murad R. Hassen; School of Electrical and Computer Engineering, AAiT, AAU, Addis Ababa, Ethiopia Graduate School of Electrical and Computer Engineering, TUT, Pretoria, SA, "Spectrum Sharing Technologies for Cognitive IoT Networks: Challenges and Future Directions", I.J. Wireless and Microwave Technologies, 2020, 1, 17-25 Published Online February 2020 in MECS(http://www.mecs-press.net) DOI: 10.5815/ijwmt.2020.01.02 Available online at http://www.mecs-press.net/ijwmt.

[15] Greg Dunko, Joydeep Misra, Josh Robertson, Tom Snyder, "A Reference Guide to the Internet of Things", Copyright © 2017 Bridgera LLC, RIoT Published by Bridgera LLC, 500 West Peace Street, Raleigh, NC 27603.

[16] Xiantao Sun, Qi Wang, Leonard J. Cimini, Larry J. Greenstein, and Douglas S. Chan, "ICI/ISI-Aware Beamforming for MIMO-OFDM Wireless Systems" IEEE TRANSACTIONS ON WIRELESS COMMUNICATIONS, VOL. 11, NO. 1, JANUARY 2012.

[17] Nazanin Rastegardoost and Bijan Jabbari, " A Machine Learning Algorithm for Unlicensed LTE and WiFi Spectrum Sharing,", Department of Electrical and Computer Engineering, George Mason University, Fairfax, Virginia, 2018 IEEE International Symposium on Dynamic Spectrum Access Networks (DySPAN), 978-1-5386-5191-9/18/$31.00 ©2018 IEEE.

[18] H. Zhang, X. Chu, W. Guo, and S. Wang, "Coexistence of WiFi and heterogeneous small cell networks sharing unlicensed spectrum," IEEE Communications Magazine, vol. 53, no. 3, pp. 158–164, March 2015.

[19] J. Li, X. Wang, D. Feng, M. Sheng, and T. Q. S. Quek, "Share in the commons: Coexistence between LTE unlicensed and WiFi," IEEE Wireless Communications, vol. 23, no. 6, pp. 16–23, December 2016.

[20] OFDM for LTE, WIFI and WIMAX Coherent versus Non-Coherent and Cooperative Turbo-Transceivers by L. Hanzo, J. Akhtman, M. Jiang, L. Wang UNIVERSITY OF SOUTHAMPTON

[21] Bolcskei, H.; ETH Zurich "MIMO-OFDM wireless systems: Basics, Perspectives, and challenges" IEEE TRANSACTIONS ON WIRELESS COMMUNICATIONS, VOL. 13, NO. 4, AUGUST 2006

[22] M.Borgmann and H. Bölcskei, "On the Capacity of Noncoherent Wideband MIMO-OFDM Systems," IEEE Int'l. Symp. Info. Theory, Adelaide, Australia, Sept. 2005, pp. 651–55.

[23] Gary Boudreau, John Panicker, Ning Guo, Rui Chang, Neng Wang, and Sophie Vrzic, Nortel, "Interference Coordination and Cancellation for 4G Networks" IEEE Communications Magazine • April 2009.

[24] Dake Liu, Coresonic AB and Linköping University Anders Nilsson and Eric Tell, Coresonic AB Di Wu and Johan Eilert, Linköping University, "Bridging Dream and Reality:Programmable Baseband Processors for Software-Defined Radio" IEEE Communications Magazine • September 2009.

[25] Anna Larmo, Magnus Lindström, Michael Meyer, Ghyslain Pelletier, Johan Torsner, and Henning Wiemann, Ericsson Research, "The LTE Link-Layer Design" IEEE Communications Magazine • April 2009.

[26] David Astély, Erik Dahlman, Anders Furuskär, Ylva Jading, Magnus Lindström, and Stefan Parkvall, Ericsson Research, "LTE: The Evolution of Mobile Broadband" IEEE Communications Magazine • April 2009.

[27] Klaus Ingemann Pedersen, Troels Emil Kolding, Frank Frederiksen, István Zsolt Kovács, Daniela Laselva, and Preben Elgaard Mogensen, Nokia Siemens Networks, "An Overview of Downlink Radio Resource Management for UTRAN Long-Term Evolution" IEEE Communications Magazine • July 2009.

[28] G. Giannattasio, J. Erfanian, P. Wills, H. Nguyen, T. Croda, K. Rauscher, X. Fernando, N. Pavlidou "Wireless Engineering Body of Knowledge" 2008 Edition; IEEE Communications Society.

[29] Wei Zhang, Xiang-Gen Xia, Khaled Ben Letaief, "Space-time/frequency coding for MIMO-OFDM in next generation broadband wireless systems" IEEE Transactions on Wireless Communications, Vol. 14, no. 3, June 2007, pp. 32-43.

[30] Hongwei Yang, Alcatel Shanghai Bell Co., Ltd., "A Road to Future Broadband Wireless Access: MIMO-OFDM-Based Air Interface" IEEE Communications Magazine • January 2005.